Journal of Neurology (2023) 270:1823–1834
https://doi.org/10.1007/s00415-022-11543-8

ORIGINAL COMMUNICATION

Brain positron emission tomography (PET) and cognitive abnormalities one year after COVID-19

Roberta Ferrucci[1,2] · Luca Cuffaro[2] · Antonella Capozza[3] · Chiara Rosci[2] · Natale Maiorana[1] · Elisabetta Groppo[2] · Maria Rita Reitano[2] · Barbara Poletti[4] · Nicola Ticozzi[4,5] · Luca Tagliabue[3] · Vincenzo Silani[4,5] · Alberto Priori[1,2]

Received: 5 September 2022 / Revised: 19 December 2022 / Accepted: 20 December 2022 / Published online: 24 January 2023

Abstract

Emerging evidence indicates that the etiologic agent responsible for coronavirus disease 2019 (COVID-19), can cause neurological complications. COVID-19 may induce cognitive impairment through multiple mechanisms. The aim of the present study was to describe the possible neuropsychological and metabolic neuroimaging consequences of COVID-19 12 months after patients' hospital discharge. We retrospectively recruited 7 patients (age [mean ± SD] = 56 years ± 12.39, 4 men) who had been hospitalized for COVID-19 with persistent neuropsychological deficits 12 months after hospital discharge. All patients underwent cognitive assessment and brain (^{18}F-FDG) PET/CT, and one also underwent ^{18}F-amyloid PET/CT. Of the seven patients studied, four had normal glucose metabolism in the brain. Three patients showed various brain hypometabolism patterns: (1) unilateral left temporal mesial area hypometabolism; (2) pontine involvement; and (3) bilateral prefrontal area abnormalities with asymmetric parietal impairment. The patient who showed the most widespread glucose hypometabolism in the brain underwent an ^{18}F-amyloid PET/CT to assess the presence of Aβ plaques. This examination showed significant Aβ deposition in the superior and middle frontal cortex, and in the posterior cingulate cortex extending mildly in the rostral and caudal anterior cingulate areas. Although some other reports have already suggested that brain hypometabolism may be associated with cognitive impairment at shorter intervals from SarsCov-2 infection, our study is the first to assess cognitive functions, brain metabolic activity and in a patient also amyloid PET one year after COVID-19, demonstrating that cerebral effects of COVID-19 can largely outlast the acute phase of the disease and even be followed by amyloid deposition.

Keywords COVID-19 · ^{18}F-amyloid PET/CT · Long COVID · Cognitive function · Hypometabolism

Introduction

SarsCov-2 infection typically induces respiratory symptoms. Emerging evidence indicates that the etiologic agent responsible for coronavirus disease 2019 (COVID-19), can cause neurological complications. [1]. Other Coronaviruses can be linked to neurological symptoms with impairment in sensory, motor and cognitive functions [2–4]. Although several pathological mechanisms could be involved in COVID 19 cognitive impairment [5], its pathophysiology remains unknown [6]. Patients with acute COVID-19 often develop, dyspnea, hypoxia, respiratory failure, and multiorgan dysfunction [7]. Conditions such as hypoxia or vascular coagulopathy can contribute to neuronal damage, and neuroinflammation can compromise the brain-blood barrier thereby increasing central nervous system cytokine levels, thus causing microglial activation and oxidative stress, eventually leading to cognitive impairment [5, 8–10]. The cognitive

Roberta Ferrucci and Luca Tagliabue contributed equally to the work.

✉ Alberto Priori
alberto.priori@unimi.it

1 Department of Health Science, Aldo Ravelli Research Center, University of Milan, Milan, Italy

2 Neurology Unit, ASST-Santi Paolo e Carlo Hospital, Milan, Italy

3 Nuclear Medicine Unit, ASST-Santi Paolo e Carlo Hospital, Milan, Italy

4 Department of Neurology and Laboratory of Neuroscience, IRCCS Auxologico Institute, Milan, Italy

5 Department of Pathophysiology and Transplantation, University of Milan, Milan, Italy

consequences of COVID-19 include impairment in multiple cognitive domains, such as executive functions, processing speed, memory, and language [4, 11–14]. COVID-19 symptoms can last several months after hospitalization, as described in the long COVID syndrome [15]. In our previous study [16] we showed that cognitive impairment can persist after 1 year. In patients with persisting cognitive impairment, more detailed information is needed on how COVID-19 progresses in the long-term. To complement clinical and neuropsychological findings, brain ^{18}F-fluorodeoxy-glucose positron emission tomography (FDG-PET) is a sensitive neuroimaging technique that can detect brain function related to cognitive function [17]. Evidence obtained in recent years indicates that brain hypometabolism patterns and cognitive impairment are associated in patients after a maximum of 6 months after the COVID-19 onset [12, 18].

In this study, we present cognitive and brain PET data from 7 patients to describe the possible neuropsychological and metabolic neuroimaging consequences of COVID-19 12 months after hospital discharge. We also report for the first time the findings obtained in one patient with ^{18}F-amyloid PET/CT.

Materials and methods

We retrospectively recruited 7 patients (age [mean ± SD] = 56years ± 12.39, 4 men) who had been hospitalized for COVID-19 between February and April 2020, in the ASST Santi Paolo e Carlo university hospitals, in Milan, Italy, and in whom neuropsychological deficits persisted 12 months after hospital discharge. Patients underwent neuropsychological assessments 5 months (T1; 158 days ± 45.24) and 12 months (T2; 363 days ± 72.21) after hospital discharge using the Brief Repeatable Battery of Neuropsychological Tests (BRB-NT) [19]. Patients who did not meet criteria for a diagnosis of dementia but showing persisting deficit in at least one of the BRB-NT battery at T2 were eligible for the participation in the study. All patients showed clinical deficits in at least two cognitive tests in the BRB-NT battery at T1 and in one cognitive test at T2. The deficit was defined by a score of two standard deviations below the normative means, corrected according to the patient's age and education level. The main deficits persisted at T2 were in the domains of verbal memory, processing and visual attention and visuospatial memory. None of the patients had neurological or psychiatric conditions that could account for the persistence of cognitive deficit at T2. None of the patients had diabetes or metabolic disorder which could interfere with neuropsychological performance measured by the BRB-NT battery. None of the patients had history of neuropsychological or psychiatric disorders previous to Sars-Cov-2 infection as reported by clinical records.

We also assessed depressive symptoms with Beck Depression Inventory-II (BDI-II) [20].

Demographic and clinical data were collected to describe patients' features and their clinical course (Table 1). All participants provided written informed consent to participate in the study. All patients met the eligibility criteria for brain ^{18}F-FDG PET/CT, in accordance with the European guidelines protocol [21, 22], and were evaluated at T2.

^{18}F-FDG PET/CT imaging

PET/CT scans were obtained according to the European procedure guidelines [21, 22]. Patients fasted for a minimum of 6 h and blood glucose levels were checked as below 200 mg/dl [23] before intravenously injecting 3.7 MBq/kg of ^{18}F-FDG. ^{18}F-FDG was administered in a quiet room, with diminished lighting and at least 10 min after the intravenous access was placed. No patient required sedation. PET/CT images were acquired about 30 to 45 min after the injection. A Discovery STE (GE Healthcare, Pewaukee, WI, USA) scanner was used for PET/CT imaging; images were acquired with a 256 × 256 matrix; scans lasted 15 min per

Table 1 Sociodemographic and clinical characteristics of the 7 patients with cognitive impairment one year after COVID-19

Subjects	Sex	Age (years)	Hospitalization duration (days)	Oxygen therapy	P/F ratio	Hyposmia/Dysgeusia
1	F	58	23	NIV	305	Hyposmia/Dysgeusia
2	M	50	6	NIV		Hyposmia/Dysgeusia
3	M	65	8	None	329	Hyposmia
4	M	55	4	Low-flow	324	None
5	F	56	8	Low-flow	275	Hyposmia/Dysgeusia
6	F	54	11	Low-flow	333	Hyposmia/Dysgeusia
7	M	55	5	Low-flow	329	Hyposmia/Dysgeusia

M male, *F* female, *P/F ratio* PaO2/FiO2 ratio, *NIV* non-invasive ventilation

bed Images were assessed by two nuclear medicine physicians, blinded to clinical information.

Images were reviewed and analyzed using Advantage Workstation (GE Healthcare) with dedicated clinical software (CortexID Suite). The reference region chosen for normalizing image intensity was the cerebellum.

PET/CT images were first evaluated qualitatively, searching for decreased or abnormal areas of FDG uptake and, eventually, their corresponding anatomic alterations in CT slices. Subsequently, we also analyzed data quantitatively. The regional glucose metabolic rate was estimated, and the entity of pathological findings was compared with data from age-matched normal controls. Data were quantified as deviations from normal values (*Z*-scores) and anatomically adjusted regions of interest.

Results were interpreted along with the visual inspection and were considered abnormal if they were ≥ 2 *Z*-scores below normative data obtained from healthy age-matched controls.

Presented data were obtained through a comparison of our population with normal databases for FDG PET imaging. The comparison was performed using an imaging software (GE CortexID Suite software), that has been developed to aid physicians in the evaluation of patient pathologies via assessment and quantification of PET brain scans [24]. The software aids in the assessment of human brain PET scans enabling automated analysis through quantification of tracer uptake and comparison with the corresponding tracer uptake in normal subjects.

The resulting quantification is presented using 3D stereotactic surface projection maps of the brain, allowing the generation of information regarding relative changes in PET-FDG glucose metabolism. The demographic characteristics of the control groups are not reported, as they come from large databases, collected by the software provider. The"normal" database for glucose tracer is obtained from a population of > 250 subjects.

^{18}F-amyloid PET/CT

PET/CT scans were acquired following the Society of Nuclear Medicine and Molecular Imaging (SNMMI) practice guidelines [25]. No specific patient preparation nor drug withdrawal was required. ^{18}F-flutemetamol was injected using a short intravenous catheter to minimize eventual adsorption of radiopharmaceutical adsorption to the catheter. 185 MBq (5 mCi) radiotracer was administered as a single i.v. slow bolus (approximately 40 s) in a total maximum 10 mL volume, followed by a 5–10 mL 0.9% sterile sodium chloride flush to ensure full dose delivery. Sedation was not required. PET/CT images were acquired approximately 90 min after the injection. PET/CT images were acquired with a Discovery STE (GE Healthcare, Pewaukee, WI, USA) scanner using a 256 × 256 matrix; scans lasted 20 min per bed. Images were assessed by two nuclear medicine physicians, trained and certified to interpret and report on amyloid-PET scans. Both nuclear medicine physicians were blinded to clinical information.

Neither the Centiloid method, nor other semi-quantitative analysis, were applied.

18F-flutemetamol PET/CT was performed in a clinical setting, therefore the scans were assessed only qualitatively, since it is the only approved method for the assessment of amyloid pathology for supporting diagnosis using PET images.

Images visual read was performed as described in the product label of amyloid PET tracer.

To this end, visual read has been validated against neuropathological determinations of amyloid burden [26].

Images were reviewed and analyzed using Advantage Workstation (GE Healthcare). Imaging quality was assessed using pons uptake as a reference region for normalizing intensity. Qualitative data were acquired by searching for an area of increased or abnormal ^{18}F-amyloid uptake. Physicians assessed the presence of anatomic alterations and cerebral atrophy in CT slices.

Results

Study population

Our study population mainly comprised men patients (4/7); the mean age was 56 ± 12.39 (mean ± SD) years and most participants ($n = 5$) had at least 8 years education. On average, patients were hospitalized for 12 days (12 ± 7.81), and the mean viral clearance time was about 1 month (28 ± 6.80 days). No patients during COVID 19 had severe acute respiratory distress syndrome ARDS (P/F ratio < 100) [28], and only 1 experienced mild ARDS (P/F ratio 200–300).

At T1, 6 of our 7 patients reported hyposmia or dysgeusia, and 5 of them reported experiencing both symptoms. At T2, no patient-reported hyposmia, whereas two reported dysgeusia. Only one patient showed symptoms of clinical depression by scoring 32 on BDI at T1 and 39 at T2 (severe: score ≥ 29).

Neuropsychological assessment

At T1, 6/7 patients (86%) showed main impairment in verbal memory, processing speed, and visual attention; 5/7 patients (71%) showed impairment in visuospatial learning and 4/7 (57%) delayed visuospatial recall.

At T2, patients' visuospatial learning had completely recovered, but 5/7 still presented verbal memory deficits (71%, 3 with stable profile, 1 worsened and 1 improved), 4/7 patients still exhibited processing and visual attention deficits (57%, all improved), 2/7 still had attention deficits (28%, both worsened), and 3/7 patients still had visual-spatial memory deficits (43%, 2 with a stable profile, 1 worsened). In one patient only, the verbal fluency deficit persisted (Table 2).

The Spearman test used to evaluate a possible correlation between demographic (age, gender, education), clinical characteristics (viral clearance time, days of hospitalization, duration of disease) and cognitive test showed a negative correlation between viral clearance time (in days) and SRT-LTS [r(7) = − 0.886 $p = 0.019$; SRT-D r (7) = − 0.820 $p = 0.046$]. We also found a negative correlation between days of hospitalization and SRT-CLTR $r(7) = 0.757$ $p = 0.049$ and with WLG $r(7) = -0.811$ $p = 0.027$, indicating that a longer infection duration and hospitalization affects cognitive performance.

^{18}F-FDG PET/CT

Deviation from normal values (*Z*-score) was deemed either statistically significant or non-significant with a cut-off -2.0.

Descriptively, we observed the lowest mean *Z*-scores (mean [min.; max.]) bilaterally in the prefrontal medial areas (right = − 0.72 [− 2.27; + 0.32]; left = − 0.59 [− 2.12; + 0.25]) and temporal mesial areas (right = − 0.50 [− 1.69; + 0.89]; left = − 0.74 [− 2.85; + 0.73]). Negative mean *Z*-scores were also observed bilaterally in lateral temporal areas (right = − 0.24 [− 1.61; + 0.75]; left = − 0.42 [− 1.61; + 0.75]), in the posterior cingulate area (right = − 0.39 [− 2.00; + 0.42]; left = − 0.21 [− 1.95; + 0.66]), and in the precuneus (right = − 0.32 [− 2.23; + 0.51]; left = − 0.15 [− 2.18; + 0.99]) (Table 3). Using a cut-off of -2.0 SD, of the seven patients, four (57%) had normal glucose cerebral metabolism (Fig. 1), whereas three patients had abnormal findings. Because none of the patients presented morphological features that could explain the deficient tracer uptake the findings were deemed to indicate regions of cortical hypometabolism.

One patient's scan showed significant frontal hypometabolism, associated with asymmetric parietal impairment and bilateral precuneus involvement, one patient presented pontine region involvement, and the last pathologic finding was a limited but significant hypometabolism, unilaterally localized in the left mesial temporal cortex (Fig. 2). Because this last patient presented the most severe glucose metabolism impairment, he was further evaluated with 18F-amyloid PET/CT. The following paragraph reports his clinical history and management.

^{18}F-amyloid PET/CT case presentation

A 65-year-old man in our sample was hospitalized for a clinical syndrome suggesting COVID-19. He had no history of behavioral or cognitive impairment. After discharge, neurocognitive assessment revealed a Montreal Cognitive Assessment test of 26.11/30 at T1 and 23.11/30 at T2. Neuropsychological assessment at T1 disclosed a deficit in SPART (10.62), SDMT (29.53), SPART-D (3.56) and SRT-D (4.88), whereas at T2 SDMT (37.53), SRT-D (4.88) and WLG (14.88), showed that processing speed and verbal memory were still impaired one year after hospital discharge and verbal fluency had even worsened.

The patient also had depressive symptoms: BDI-II = 11 at T1 indicating minimal symptoms, and BDI-II = 20 at T2 indicating moderate symptoms. Because clinical assessment suggested a progressive neurocognitive impairment, the

Table 2 Results of the cognitive assessments at 5 (T1) and 12 (T2) months after COVID-19

Subjects	SRT-LTS cut-off ≥ 23.3		SRT-CLTR (cut-off ≥ 15.5)		SPART (cut-off ≥ 12.7)		SDMT (cut-off ≥ 37.9)		PASAT-3 (cut-off ≥ 28.4)		PASAT-2 (cut-off ≥ 17.01)		SRT-D (cut-off ≥ 4.9)		SPART-D (cut-off ≥ 3.6)		WLG (cut-off ≥ 17.0)	
	T1	T2	T1	T2	T1	T2	T1	T2	T1	T2	T1	T2	T1	T2	T1	T2	T1	T2
1	27.55	18.55	5.91	3.91	10.31	12.31	24.27	30.27	16.19	14.19	13.87	6.87	3.08	3.08	4.41	5.41	22.88	21.88
2	29.16	34.16	23.07	34.07	11.78	17.78	37.38	36.38	47.98	48.98	37.33	39.33	7.88	4.88	1.92	7.92	34.12	27.12
3	35.17	26.17	23.78	19.78	10.62	20.62	29.53	37.53	51.47	51.47	26.91	28.91	4.88	4.88	3.56	5.56	26.12	30.12
4	25.16	46.16	19.07	38.07	10.78	17.78	27.38	35.38	36.98	36.98	31.33	28.33	4.88	6.88	3.92	2.92	30.12	34.12
5	19.55	2.55	12.91	1.91	14.31	5.31	30.27	39.27	41.19	45.19	27.87	27.87	3.08	3.08	3.41	3.41	24.88	24.88
6	30.17	41.17	24.78	23.78	11.62	15.62	40.53	45.53	21.47	22.47	15.91	14.91	4.88	5.88	3.56	3.56	17.88	14.88
7	31.16	36.16	17.07	27.07	16.78	19.78	34.38	45.38	51.98	55.98	33.33	36.33	1.88	4.88	4.92	5.92	27.12	29.12

SRT-LTS serial recall test long term storage, *SRT-CLTR* serial recall test consistent long-term retrieval, *SPART* spatial recall test, *SDMT* symbol digit modalities test, *PASAT-2* paced serial additions test (2 s interval), *PASAT-3* paced serial addition test (3 s interval), *SRT-D* serial recall test delayed recall, *SPART-D* spatial recall test delayed, *WLG* word list generation. Data shown in bold represent scores below the test cut-off

Table 3 *Z*-score values for each cortical region per patient. Data were acquired by analyzing semi-quantitative data on ^{18}F-FDG PET/CT imaging

Brain area	1 (58. F)	2 (50. M)	3 (65. M)	4 (55. M)	5 (56. F)	6 (54. F)	7 (55. M)	Mean	SD
Right lateral prefrontal	0.51	1.01	0.28	− 0.89	1.23	− 2.22	− 0.73	− 0.12	1.23
Left lateral prefrontal	0.43	1.19	0.27	− 0.61	0.65	− 2.30	− 0.73	− 0.16	1.16
Right prefrontal medial	0.09	0.32	− 1.09	− 0.93	− 0.23	− 2.27	− 0.96	− 0.72	0.88
Left prefrontal medial	0.02	0.25	− 0.85	− 0.78	0.08	− 2.12	− 0.76	− 0.59	0.82
Right sensorimotor	0.37	1.05	0.95	− 0.64	0.82	− 1.73	0.22	0.15	1.01
Left sensorimotor	0.06	0.80	0.16	− 0.35	0.62	− 1.98	0.70	0.00	0.96
Right anterior cingulate	1.08	0.63	− 0.83	− 0.02	0.61	− 0.64	0.48	0.19	0.71
Left anterior cingulate	0.83	0.69	− 0.43	0.21	0.54	− 0.63	0.21	0.20	0.55
Right posterior cingulate	0.42	0.20	− 0.48	− 0.99	0.20	− 2.00	− 0.10	− 0.39	0.86
Left posterior cingulate	0.58	0.66	− 0.09	− 0.68	0.36	− 1.95	− 0.32	− 0.21	0.91
Right precuneus	0.51	0.19	0.22	− 1.04	0.43	− 2.23	− 0.32	− 0.32	1.00
Left precuneus	0.55	0.99	0.00	− 0.69	0.38	− 2.18	− 0.07	− 0.15	1.04
Right superior parietal	1.06	− 0.04	0.52	− 0.49	0.58	− 1.46	0.76	0.13	0.87
Left superior parietal	0.94	− 0.13	− 0.78	− 0.50	− 0.02	− 2.25	1.49	− 0.18	1.21
Right inferior parietal	1.17	0.40	− 0.21	− 1.11	1.04	− 1.69	− 0.23	− 0.09	1.06
Left inferior parietal	0.55	0.61	− 0.67	− 0.64	0.98	− 2.13	− 0.21	− 0.22	1.06
Right lateral occipital	1.42	1.32	0.66	− 0.04	1.32	− 1.67	0.61	0.52	1.10
Left lateral occipital	1.27	1.23	0.60	0.18	1.37	− 1.75	0.97	0.55	1.10
Right primary visual	2.60	1.70	1.39	0.00	0.75	− 1.74	2.73	1.06	1.57
Left primary visual	2.04	1.44	1.00	− 0.23	1.27	− 1.81	2.44	0.88	1.46
Right lateral temporal	0.35	0.65	− 0.45	− 0.97	0.99	− 1.61	− 0.67	− 0.24	0.94
Left lateral temporal	− 0.10	0.49	− 1.11	− 0.72	0.75	− 1.61	− 0.62	− 0.42	0.85
Right temporal mesial	0.02	0.89	− 1.69	− 0.81	0.02	− 0.58	− 1.33	− 0.50	0.88
Left temporal mesial	− 0.41	0.73	− 2.85	− 0.72	0.09	− 0.93	− 1.07	− 0.74	1.12
Pons	− 2.13	2.68	− 1.83	− 0.54	0.71	0.25	0.16	− 0.10	1.63

Patients' quantified uptake was compared with reference values obtained from healthy age-matched controls. Deviation from normal values was deemed either statistically significant or non-significant using a -2 SD cut-off

patient was referred to the Nuclear Medicine Unit to assess his brain glucose metabolism status, using ^{18}F- FDG PET/CT. Scans (Fig. 3, Table 4) showed a significant reduction in FDG uptake in the left mesial temporal cortex. Owing to the severe hypometabolism despite its limited extension, the ^{18}F-FDG PET/CT scan was reported as inconclusive, because it failed to identify a typical hypometabolic pattern and diagnose neurodegenerative disease. The patient therefore underwent an ^{18}F-amyloid PET/CT scan to check for Aβ plaques. ^{18}F-flutemetamol PET/CT showed significant Aβ deposition in the superior and middle frontal cortex, in the posterior cingulate (Fig. 4), and, to a lesser extent, in the rostral and caudal anterior cingulate areas. At 1-year follow-up, the patient remained neuropsychologically stable without receiving acetylcholinesterase inhibitors.

Discussion

Our findings confirm that cognitive abnormalities can detect 12 months after patients have COVID-19 and in many cases (42.8% in our sample) these are associated with abnormal brain metabolism. Brain hypometabolism patterns differed, and selectively involved the left temporal mesial area, pontine area, and bilaterally the prefrontal and parietal areas. In all patients, neuropsychological tests to check for cognitive deficits improved slightly, but at least one cognitive test in the BRB-NT battery remained deficient. Although some other studies conducted at shorter intervals after SarsCov-2 infection have reported brain hypometabolism may be associated with cognitive impairment, in our study we assessed cognitive functions

Reference Region Cerebellum – whole		
Cortical region	Patient	Z-score
Prefrontal Lateral R	1,42	1,01
Prefrontal Lateral L	1,45	1,19
Prefrontal Medial R	1,25	0,32
Prefrontal Medial L	1,26	0,25
Sensorimotor R	1,35	1,05
Sensorimotor L	1,34	0,80
Anterior Cingulate R	1,19	0,63
Anterior Cingulate L	1,19	0,69
Posterior Cingulate R	1,44	0,20
Posterior Cingulate L	1,49	0,66
Precuneus R	1,42	0,19
Precuneus L	1,51	0,99
Parietal Superior R	1,24	-0,04
Parietal Superior L	1,21	-0,13
Parietal Inferior R	1,33	0,40
Parietal inferior L	1,35	0,61
Occipital Lateral R	1,44	1,32
Occipital Lateral L	1,42	1,23
Primary Visual R	1,62	1,70
Primary Visual L	1,61	1,44
Temporal Lateral R	1,21	0,65
Temporal Lateral L	1,20	0,49
Temporal Mesial R	0,92	0,89
Temporal Mesial L	0,91	0,73
Cerebellum Whole	1,00	0,00
Pons	0,89	2,68

Fig. 1. ^{18}F-FDG PET/CT elaboration using dedicated clinical software (CortexID Suite – GE Healthcare). The cerebellum was chosen as the reference region for intensity normalization. The table on the right reports the regional quantitative results: it shows the quantification of radiopharmaceutical uptake in the patient (left column). and its value assessed in terms of deviations from normal (*Z*-scores) (right column). The patient presented normal glucose cerebral metabolism (Patient number 2). The upper panel shows the 3D SSP map of FDG uptake in the specific patient (Sokoloff scale reported on the left). The lower panel is a 3D-SSP Z-score image that shows no significant deviation from normal group

and brain metabolic activity 1 year after COVID-19, thus demonstrating that cerebral effects can largely outlast the acute phase of disease. In a study enrolling 29 COVID-19 patients in the subacute stage of disease (from two to five weeks after the onset), Hosp et al. [12] included subjects without a history of cognitive deficit or degenerative disease. Most of them showed altered taste or smell or both, Montreal Cognitive Assessment (MoCA) performance was impaired in 18/26 patients and ^{18}FDG-PET disclosed pathological results in 10/15 patients with predominant frontoparietal hypometabolism [12]. The same authors prospectively assessed the MoCA and ^{18}FDG-PET scans for 8 of COVID-19 patients at a chronic stage of infection (6 months after the onset) and reported a significant reduction in the initial frontoparietal and, to a lesser extent, temporal hypometabolism that correlated inversely with MoCA performance [18]. In their report, Guedj et al. [2], described brain ^{18}F-FDG PET hypometabolism in 35 patients at least 3 weeks after initial infection. Compared with healthy subjects, the patients showed hypometabolism in the bilateral orbital gyrus, including the olfactory gyrus, and in the connected structures

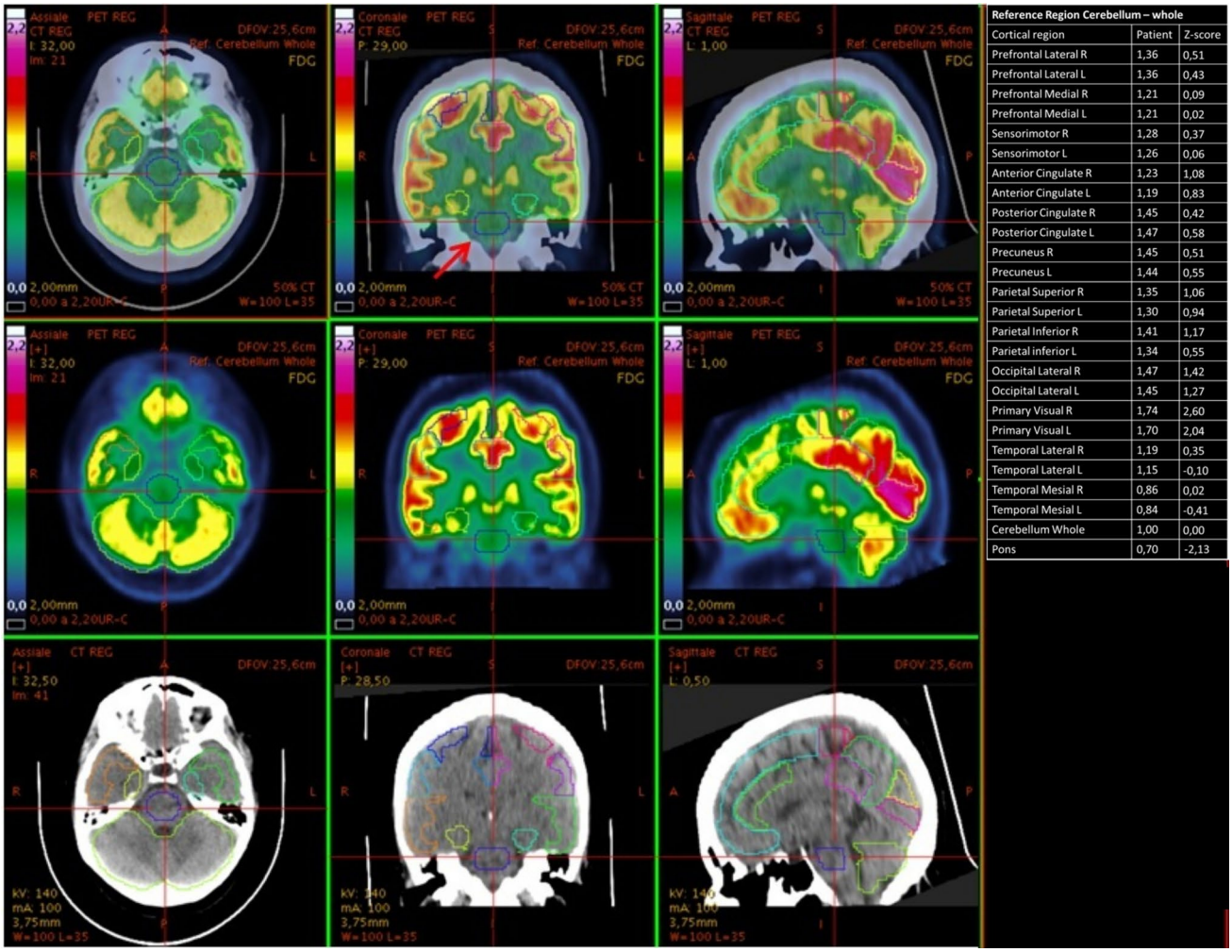

Reference Region Cerebellum – whole		
Cortical region	Patient	Z-score
Prefrontal Lateral R	1,36	0,51
Prefrontal Lateral L	1,36	0,43
Prefrontal Medial R	1,21	0,09
Prefrontal Medial L	1,21	0,02
Sensorimotor R	1,28	0,37
Sensorimotor L	1,26	0,06
Anterior Cingulate R	1,23	1,08
Anterior Cingulate L	1,19	0,83
Posterior Cingulate R	1,45	0,42
Posterior Cingulate L	1,47	0,58
Precuneus R	1,45	0,51
Precuneus L	1,44	0,55
Parietal Superior R	1,35	1,06
Parietal Superior L	1,30	0,94
Parietal Inferior R	1,41	1,17
Parietal inferior L	1,34	0,55
Occipital Lateral R	1,47	1,42
Occipital Lateral L	1,45	1,27
Primary Visual R	1,74	2,60
Primary Visual L	1,70	2,04
Temporal Lateral R	1,19	0,35
Temporal Lateral L	1,15	-0,10
Temporal Mesial R	0,86	0,02
Temporal Mesial L	0,84	-0,41
Cerebellum Whole	1,00	0,00
Pons	0,70	-2,13

Fig. 2. ^{18}F-FDG PET/CT elaboration using dedicated clinical software (CortexID Suite – GE Healthcare). The cerebellum was chosen as the reference region for intensity normalization. The table on the right reports the quantification of radiopharmaceutical uptake. assessed in terms of deviations from normal values (*Z*-scores) in specific regions of interest. As shown by the table. the patient (Patient number 1) presented a hypometabolic pontine area. with a *Z*-score value of − 2.13 compared to healthy age-matched controls. The images panels show. from left to right. the axial. Coronal and sagiptal views; and from top to bottom PET/CT co-registration images. PET-only images and CT-only images. PET images are depicted in Sokoloff scale. The cursor (and the red arrow in the upper middle panel) points on the pontine pathologic area

in the medial temporal lobe, brainstem, and cerebellum [2]. Kas et al. [3] reported widespread hypometabolism in COVID patients including the frontal cortex, anterior cingulate, insula, and caudate nucleus in the subacute phase (1 month), which partially improved at 6 months, although prefrontal, insular and subcortical abnormalities persisted [3]. We collected neuropsychological data until one year after the onset of neurological symptoms, correlating them with FDG-PET findings and even analyzing the brain Aβ deposition via ^{18}F-amyloid PET/CT in one case. Our results support the proposed correlation between brain hypometabolism and lasting cognitive deficits in COVID-19 patients one year after the infection. We found a heterogeneous pattern of abnormalities variably affecting prefrontal, temporal-mesial, parietal and pontine areas, those more affected during SARS-CoV-2 [27–29] infection. However, in our sample not all patients who had cognitive deficits showed hypometabolism as measured by FDG-PET. This result are similar to findings from other authors [30] showing cognitive impairment without significant decline in FDG-PET metabolism [31] Monitoring the advancement of hypometabolism in the brain

Reference Region Cerebellum – whole		
Cortical region	Patient	Z-score
Prefrontal Lateral R	1,29	0,28
Prefrontal Lateral L	1,28	0,27
Prefrontal Medial R	1,06	-1,09
Prefrontal Medial L	1,08	-0,85
Sensorimotor R	1,30	0,95
Sensorimotor L	1,22	0,16
Anterior Cingulate R	0,96	-0,83
Anterior Cingulate L	1,00	-0,43
Posterior Cingulate R	1,28	-0,48
Posterior Cingulate L	1,32	-0,09
Precuneus R	1,37	0,22
Precuneus L	1,32	0,00
Parietal Superior R	1,25	0,52
Parietal Superior L	1,06	-0,78
Parietal Inferior R	1,20	-0,21
Parietal inferior L	1,14	-0,67
Occipital Lateral R	1,35	0,66
Occipital Lateral L	1,33	0,60
Primary Visual R	1,56	1,39
Primary Visual L	1,51	1,00
Temporal Lateral R	1,07	-0,45
Temporal Lateral L	1,01	-1,11
Temporal Mesial R	0,75	-1,69
Temporal Mesial L	0,69	-2,85
Cerebellum Whole	1,00	0,00
Pons	0,72	-1,83

Fig. 3. ^{18}F-FDG PET/CT elaboration using dedicated clinical software (CortexID Suite – GE Healthcare). The cerebellum was chosen as the reference region for intensity normalization. The table on the right reports the quantification of radiopharmaceutical uptake. assessed in terms of deviations from normal values (*Z*-scores) in specific regions of interest. As shown by the table. The patient (Patient number 3) presented a significant hypometabolism in the left temporal mesial area. with a *Z*-score value of − 2.85. compared to healthy age-matched controls. The upper panel shows the 3D SSP map of FDG uptake in the specific patient (Sokoloff scale reported on the left). The lower panel is a 3D-SSP *z*-score image that shows a significant deviation from age-matched controls in the left temporal mesial area (the golden-brown area pointed by the blue arrow)

with PET in case of persistent cognitive decline could help to discriminate between dementia and reversible cognitive impairment due to acute COVID infection [32]. To date no published study has used an ^{18}F-amyloid PET/CT scan after COVID-19. In our study, one patient, due to the severe hypometabolism, underwent an ^{18}F-amyloid PET/CT that showed significant Aβ deposition in the superior and middle frontal cortex, in the posterior cingulate areas, and, to a lesser extent, in the rostral and caudal anterior cingulate cortices.

There is an association between neurodegenerative proteinopathies and neuroinfections [33]. Infectious agents, like viruses, could be involved in the pathogenesis of Alzheimer's disease [34]. They might be able to evade the host immune system leading to chronic infection, inflammation, and subsequent Aβ and phosphorylated-tau deposition in the brain. [33]

Strong evidence suggests a potential SarsCov-2 role in the pathogenesis of neurological injury, as the results

Table 4 Quantification of radiopharmaceutical uptake of ^{18}F-FDG PET/CT

Brain area	Radiopharmaceutical uptake	*Z*-scores
Right lateral prefrontal	1.29	0.28
Left lateral prefrontal	1.28	0.27
Right prefrontal medial	1.06	– 1.09
Left prefrontal medial	1.08	– 0.85
Right sensorimotor	1.30	0.95
Left sensorimotor	1.22	0.16
Right anterior cingulate	0.96	– 0.83
Left anterior cingulate	1.00	– 0.43
Right posterior cingulate	1.28	-0.48
Left posterior cingulate	1.32	-0.09
Right precuneus	1.37	0.22
Left precuneus	1.32	0.00
Right superior parietal	1.25	0.52
Left superior parietal	1.06	– 0.78
Right inferior parietal	1.20	– 0.21
Left inferior parietal	1.14	– 0.67
Right lateral occipital	1.35	0.66
Left lateral occipital	1.33	0.60
Right primary visual	1.56	1.39
Left primary visual	1.51	1.00
Right lateral temporal	1.07	– 0.45
Left lateral temporal	1.01	– 1.11
Right temporal mesial	0.75	– 1.69
Left temporal mesial	0.69	– 2.85
Pons	0.72	– 1.83

^{18}F-FDG PET/CT. assessed in terms of deviations from normal values (*Z*-scores) in specific regions of interest. The left temporal mesial cortex shows a significant reduction in FDG uptake. Data elaborated using dedicated clinical software (CortexID Suite – GE Healthcare)

from UK Biobank imply [35]. They support evidence that limbic brain imaging damage may be the in vivo hallmark indicating degenerative disease spread through olfactory pathways, or neuroinflammatory events. On the same line, Ciaccio et al. [36] suggest that a disrupted blood–brain barrier (BBB) may support the SarsCov-2 neuroinvasion. Thus, the elderly could be more susceptible to neuroinvasion during infection, leading to the development of neurodegenerative diseases, including Alzheimer's disease [36].

Several studies have established a causal relationship between inflammatory state and neurodegeneration. The link appears to be based on microglial activation, leading to the production of pro-inflammatory cytokines (IL-1β, IL-6, TNF-α), which appear to be responsible for synaptic alterations and altered enzymatic processes capable of leading to cell death [36–38]. Chouhan and colleagues [39] confirmed that a sustained innate immune activation and altered expression of genes linked to synaptic plasticity may contribute to the onset or progression or both of neurodegeneration [39].

In about 5% of patients with severe disease a systemic dysregulated cytokine response develops, described as a possible causal connection between the severe systemic inflammatory reaction (cytokine storm) in COVID-19 and neurodegeneration. The pro-inflammatory cytokines involved in COVID-19 pathogenesis are reportedly the same [40]. Rau et al. [41] described the correlation between interleukin-6 (IL-6), a marker indicating the COVID-19-related inflammatory response, and cerebral white matter changes in COVID-19 patients [41]. The massive systemic pro-inflammatory cytokine release, associated with hypoxia status, may damage the blood–brain barrier, leading o inflammatory spread in the central nervous system [36, 38, 42]. A similar enzymatic pathway influenced by pro-inflammatory cytokines involves amyloid metabolism, possibly influenced by the cytokine release syndrome, leading to the development of amyloid plaques [36, 38], a key element in Alzheimer's neurodegeneration [43]. Our study has some limitations, few data on patients' antecedents were available and to date it is not possible to fully exclude the absence of cognitive impairment or brain hypometabolism before COVID-19 infection. To confirm our findings studies with larger sample sizes and follow-up over 12 months are needed.

Conclusion

Our results suggest that, in addition to cognitive changes, SarsCov-2 infection can also induce abnormalities in brain metabolism and possibly amyloid deposition that persists one year after infection.

Neurological sequelae, including the cognitive impairment leading to Alzheimer's disease might in the future be a major feature complicating COVID-19. Further studies need to explain the pathophysiological mechanisms underlying the long-term neurological consequences of SarsCov-2 infection and its possible correlation with amyloid-related cognitive impairment. From a practical viewpoint, physicians should

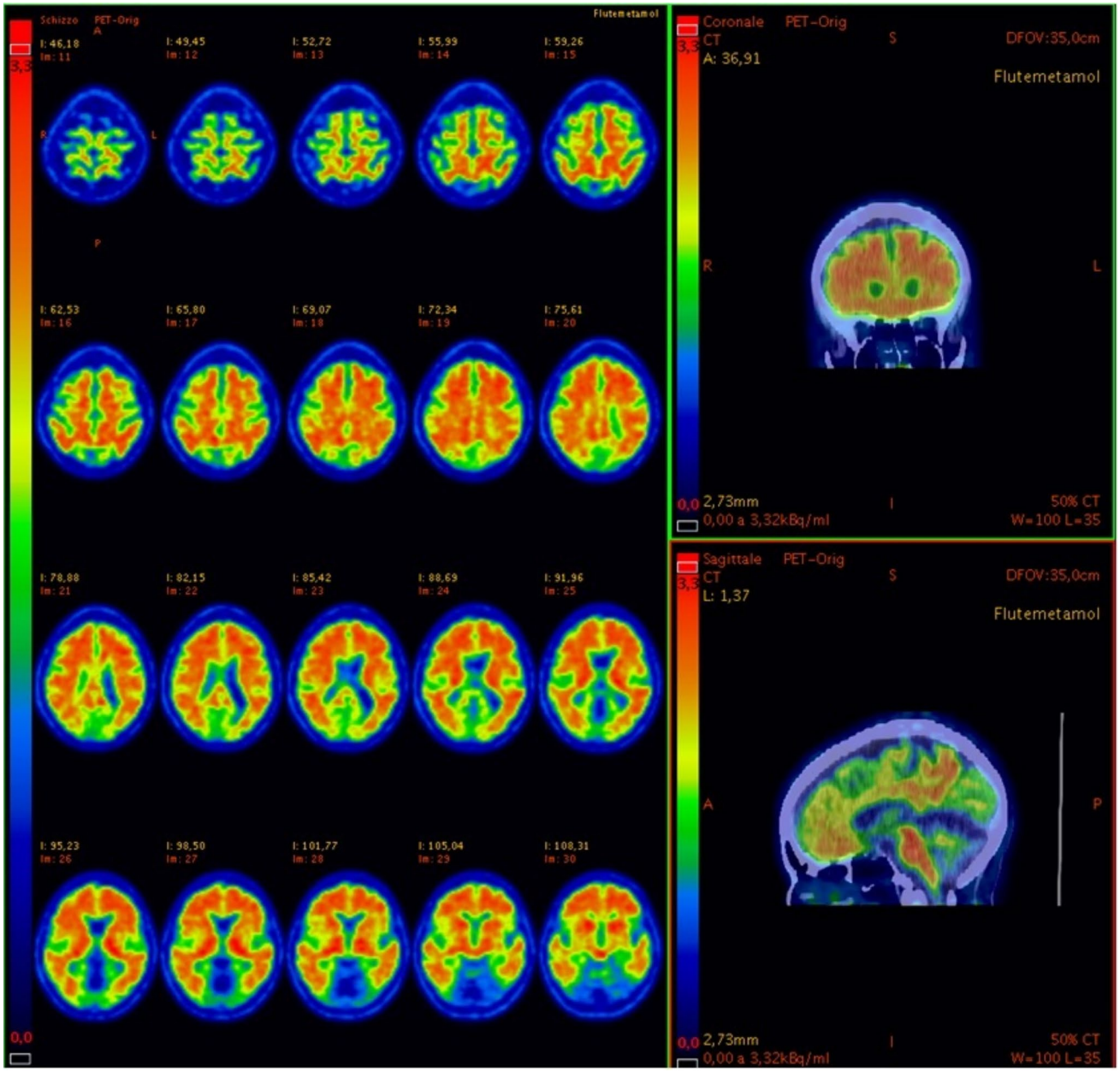

Fig. 4 ^{18}F-amyloid PET/CT in sagittal and coronal views and PET-only scan in axial views. The slices show increased saturation and abnormal uptake in the superior and middle frontal cortex. pathognomonic of Aβ plaque deposition. ^{18}F-amyloid PET/CT and PET-only scan in sagittal views. The slice shows intensity of the uptakes in the posterior cingulate. As shown on the left column in each panel. the images are presented in Rainbow scale and are adjusted according to the guidelines of.^{18}F-flutemetamol PET/TC review (e.g., the color scale to set the pons to approximately 90% maximum intensity)

always keep a COVID-19 history in mind when ^{18}F-FDG-PET detects focal brain hypometabolism or PET/CT discloses otherwise unexplained amyloid deposition.

Acknowledgements This study was partially supported by donation of the Romeo and Enrica Invernizzi Foundation. Roberta Ferrucci were supported from the Ravelli Center Research Center (CRC) for Neurotechnology and Brain Therapeutics.

Author contributions RF, AP: contributing to conception and design, analyzing and interpreting data, drafting the manuscript, approving the final content of the manuscript. LC, AC, NM, CR, EG, NT, MRR, BP, VS: analyzing and interpreting data, drafting and revising the manuscript, approving the final content of the manuscript. LT, AC: acquiring and interpreting data, drafting and revising the manuscript, approving the final content of the manuscript.

Funding No funding was received for conducting this study.

Data availability The datasets used and/or analyzed during the current study are available from the corresponding author on reasonable request.

Declarations

Conflicts of interest The authors have no relevant financial or non-financial interests to disclose.

Ethical approval IRB review board has approved the use of humans for this study (CogCov: n. 2020/ST/105, Comitato Etico Milano Area 1) and we received consent forms from any participant in a study.

Consent to participate Informed consent was obtained from all individual participants included in the study.

References

1. Priori A, Senior E, Dini M, Deputy E (2021) Neurology of COVID-19. Milano university press, Milan
2. Guedj E, Campion JY, Dudouet P, Kaphan E, Bregeon F, Tissot-Dupont H et al (2021) 18F-FDG brain PET hypometabolism in patients with long COVID. Eur J Nucl Med Mol Imaging 48:2823–33
3. Kas A, Soret M, Pyatigoskaya N, Habert M-O, Hesters A, Le Guennec L et al (2021) The cerebral network of COVID-19-related encephalopathy: a longitudinal voxel-based 18F-FDG-PET study. Eur J Nucl Med Mol Imaging. 48:2543–57
4. Miskowiak KW, Johnsen S, Sattler SM, Nielsen S, Kunalan K, Rungby J et al (2021) Cognitive impairments four months after COVID-19 hospital discharge: pattern, severity and association with illness variables. Eur Neuropsychopharmacol Elsevier B.V. 46:39–48
5. Baker HA, Safavynia SA, Evered LA (2021) The 'third wave': impending cognitive and functional decline in COVID-19 survivors. Br J Anaesth 126:44–47
6. Vijiala S, Epiney J-B, Jöhr J, Pincherle A, Meyer MM, Du Pasquier R, et al (2021) Case report: behavioral unresponsiveness in acute COVID-19 patients: the utility of the motor behavior tool-revised and (18)F-FDG PET/CT. Front Neurol 644848
7. Chen N, Zhou M, Dong X, Qu J, Gong F, Han Y et al (2020) Epidemiological and clinical characteristics of 99 cases of 2019 novel coronavirus pneumonia in Wuhan, China: a descriptive study. Lancet Elsevier Ltd 395:507–513
8. Zubair AS, McAlpine LS, Gardin T, Farhadian S, Kuruvilla DE, Spudich S (2020) Neuropathogenesis and neurologic manifestations of the coronaviruses in the age of coronavirus disease 2019: a review. JAMA Neurol 77:1018–1027
9. Song E, Zhang C, Israelow B, Lu-Culligan A, Prado AV, Skriabine S, et al (2021) Neuroinvasion of SARS-CoV-2 in human and mouse brain. J Exp Med 218(3):e20202135. https://doi.org/10.1084/jem.20202135
10. Safavynia SA, Goldstein PA (2019) The role of neuroinflammation in postoperative cognitive dysfunction: moving from hypothesis to treatment. Front Psychiatry 9:752. https://doi.org/10.3389/fpsyt.2018.00752
11. Méndez R, Balanzá-Martínez V, Luperdi SC, Estrada I, Latorre A, González-Jiménez P, et al (2021) Short-term neuropsychiatric outcomes and quality of life in COVID-19 survivors. J Intern Med 290(3):621–631. https://doi.org/10.1111/joim.13262
12. Hosp JA, Dressing A, Blazhenets G, Bormann T, Rau A, Schwabenland M et al (2021) Cognitive impairment and altered cerebral glucose metabolism in the subacute stage of COVID-19. Brain 144:1263–1276
13. Almeria M, Cejudo JC, Sotoca J, Deus J, Krupinski J (2020) Cognitive profile following COVID-19 infection: clinical predictors leading to neuropsychological impairment. Brain, Behav Immun - Heal 9:100163
14. Zhou H, Lu S, Chen J, Wei N, Wang D, Lyu H et al (2020) The landscape of cognitive function in recovered COVID-19 patients. J Psychiatr Res Elsevier Ltd 129:98–102
15. Potus F, Mai V, Lebret M, Malenfant S, Breton-Gagnon E, Lajoie AC et al (2020) Novel insights on the pulmonary vascular consequences of COVID-19. Am J Physiol - Lung Cell Mol Physiol 319:L277–L288
16. Ferrucci R, Dini M, Groppo E, Rosci C, Reitano MR, Bai F et al (2021) Long-lasting cognitive abnormalities after COVID-19. Brain Sci 11:1–11
17. Chételat G, Arbizu J, Barthel H, Garibotto V, Law I, Morbelli S et al (2020) Amyloid-PET and (18)F-FDG-PET in the diagnostic investigation of Alzheimer's disease and other dementias. Lancet Neurol England 19:951–962
18. Blazhenets G, Schröter N, Bormann T, Thurow J, Wagner D, Frings L et al (2021) Slow but evident recovery from neocortical dysfunction and cognitive impairment in a series of chronic COVID-19 patients. J Nucl Med 62:910–915
19. Amato MP, Portaccio E, Goretti B, Zipoli V, Ricchiuti L, De Caro MF et al (2006) The Rao's brief repeatable battery and stroop test: normative values with age, education and gender corrections in an Italian population. Mult Scler J Mult Scler 12:787–793
20. Arnarson PÖ, Ólason DP, Smári J, Sigurdsson JF (2009) The Beck depression inventory second edition (BDI-II): psychometric properties in Icelandic student and patient populations. Taylor & Francis 62:360–5
21. Guedj E, Varrone A, Boellaard R, Albert NL, Barthel H, van Berckel B et al (2022) EANM procedure guidelines for brain PET imaging using [18F]FDG, version 3. Eur J Nucl Med Mol Imaging 49:632–651
22. Nobili F, Arbizu J, Bouwman F, Drzezga A, Agosta F, Nestor P et al (2018) European association of nuclear medicine and european academy of neurology recommendations for the use of brain 18 F-fluorodeoxyglucose positron emission tomography in neurodegenerative cognitive impairment and dementia: Delphi consensus. Eur J Neurol 25:1201–1217
23. Eskian M, Alavi A, Khorasanizadeh MH, Viglianti BL, Jacobsson H, Barwick TD et al (2019) Effect of blood glucose level on standardized uptake value (SUV) in 18F- FDG PET-scan: a systematic review and meta-analysis of 20,807 individual SUV measurements. Eur J Nucl Med Mol Imaging 46:224–237
24. Lindström E, Oddstig J, Danfors T, Jögi J, Hansson O, Lubberink M (2020) Image reconstruction methods affect software-aided assessment of pathologies of [18F]flutemetamol and [18F]FDG brain-PET examinations in patients with neurodegenerative diseases. NeuroImage Clin. Elsevier 28:102386
25. Minoshima S, Drzezga AE, Barthel H, Bohnen N, Djekidel M, Lewis DH et al (2016) SNMMI procedure standard/EANM practice guideline for amyloid PET imaging of the brain 1.0. J Nucl Med. United States. 57:1316–22
26. Salloway S, Gamez JE, Singh U, Sadowsky CH, Villena T, Sabbagh MN et al (2017) Performance of [18F]flutemetamol amyloid imaging against the neuritic plaque component of CERAD and the current (2012) NIA-AA recommendations for the neuropathologic diagnosis of Alzheimer's disease. Assess Dis Monit 9:25–34
27. Fontana IC, Bongarzone S, Gee A, Souza DO, Zimmer ER (2020) PET imaging as a tool for assessing COVID-19 brain changes. Trends Neurosci 43:935–938
28. Duan K, Premi E, Pilotto A, Cristillo V, Benussi A, Libri I et al (2021) Alterations of frontal-temporal gray matter volume

associate with clinical measures of older adults with COVID-19. Neurobiol Stress 14:100326
29. Huang Y, Ling Q, Manyande A, Wu D, Xiang B (2022) Brain imaging changes in patients recovered from COVID-19: a narrative review. Front Neurosci 16:855868
30. Rudroff T, Workman CD, Ponto LLB (2021) ^{18}F-FDG-PET imaging for post-COVID-19 brain and skeletal muscle alterations. Viruses 13(11):2283. https://doi.org/10.3390/v13112283
31. Dressing A, Bormann T, Blazhenets G, Schroeter N, Walter LI, Thurow J et al (2022) Neuropsychologic profiles and cerebral glucose metabolism in neurocognitive long COVID syndrome.". J Nucl Med 63:1058–1063
32. Vélez M, Falconí Paez A, Nicolalde B, Esquetini-Vernon C, Lara-Taranchenko Y, Zambrano K et al (2022) Cognitive impairment or dementia in post-acute COVID-19 syndrome. Two suspects and a perfect detective: positron emission tomography (PET) scan. Eur Neuropsychopharmacol 61:91–93
33. Danics K, Forrest SL, Kapas I, Erber I, Schmid S, Törő K et al (2021) Neurodegenerative proteinopathies associated with neuroinfections. J Neural Transm 128:1551–1566
34. Fulop T, Witkowski JM, Larbi A, Khalil A, Herbein G, Frost EH (2019) Does HIV infection contribute to increased beta-amyloid synthesis and plaque formation leading to neurodegeneration and Alzheimer's disease? J Neurovirol United States 25:634–647
35. Douaud G, Lee S, Alfaro-Almagro F, Arthofer C, Wang C, McCarthy P et al (2022) SARS-CoV-2 is associated with changes in brain structure in UK Biobank. Nature 604:697–707
36. Ciaccio M, Lo Sasso B, Scazzone C, Gambino CM, Ciaccio AM, Bivona G et al (2021) COVID-19 and Alzheimer's disease. Brain Sci 11:1–10
37. Akiyama H, Barger S, Barnum S, Bradt B, Bauer J, Cole GM et al (2000) Inflammation and Alzheimer's disease. Neurobiol Aging 21:383–421
38. Webers A, Heneka MT, Gleeson PA (2020) The role of innate immune responses and neuroinflammation in amyloid accumulation and progression of Alzheimer's disease. Immunol Cell Biol United States 98:28–41
39. Chouhan JK, Püntener U, Booth SG, Teeling JL (2021) Systemic inflammation accelerates changes in microglial and synaptic markers in an experimental model of chronic neurodegeneration. Front Neurosci 15:760721
40. Darif D, Hammi I, Kihel A, El Idrissi SI, Guessous F, Akarid K (2021) The pro-inflammatory cytokines in COVID-19 pathogenesis: what goes wrong? Microb Pathog 153:104799
41. Rau A, Schroeter N, Blazhenets G, Dressing A, Walter LI, Kellner E et al (2022) Widespread white matter oedema in subacute COVID-19 patients with neurological symptoms. Oxford University Press (OUP), Brain
42. Qin Y, Wu J, Chen T, Li J, Zhang G, Wu D, et al (2021) Long-term microstructure and cerebral blood flow changes in patients recovered from COVID-19 without neurological manifestations. J Clin Invest 131
43. Murphy MP, LeVine H 3rd (2010) Alzheimer's disease and the amyloid-beta peptide. J Alzheimers Dis 19:311–323